



## High Pressure Research: An International Journal

Publication details, including instructions for authors and subscription information:

<http://www.tandfonline.com/loi/ghpr20>

### The structural and optical properties of ZnO bulk and nanocrystals under high pressure

A. Duzynska<sup>a</sup>, R. Hrubia<sup>b</sup>, V. Drozd<sup>b</sup>, H. Teisseyre<sup>a,c</sup>, W. Paszkowicz<sup>a</sup>, A. Reszka<sup>a</sup>, A. Kaminska<sup>a</sup>, S. Saxena<sup>b</sup>, J. D. Fidelus<sup>a,c</sup>, J. Grabis<sup>d</sup>, C. J. Monty<sup>e</sup> & A. Suchocki<sup>a,f</sup>

<sup>a</sup> Institute of Physics, Polish Academy of Sciences, Lotników 32/46, 02-668, Warsaw, Poland

<sup>b</sup> CeSMEC, Florida International University, University Park, Miami, FL, 33199, USA

<sup>c</sup> Institute of High Pressure Physics, Polish Academy of Science, Sokolowska 29/37, 01-142, Warsaw, Poland

<sup>d</sup> Institute of Inorganic Chemistry, Riga Technical University, 34 Miera, LV-2169, Salaspils, Latvia

<sup>e</sup> CNRS Laboratoire Procédés, Matériaux et Énergie Solaire (PROMES), Odeillo, 66120, Font-Romeu, France

<sup>f</sup> Institute of Physics, Kazimierz Wielki University, Plac Weyssenhoffa 11, 85-072, Bydgoszcz, Poland

Version of record first published: 11 Jul 2012

To cite this article: A. Duzynska, R. Hrubia, V. Drozd, H. Teisseyre, W. Paszkowicz, A. Reszka, A. Kaminska, S. Saxena, J. D. Fidelus, J. Grabis, C. J. Monty & A. Suchocki (2012): The structural and optical properties of ZnO bulk and nanocrystals under high pressure, High Pressure Research: An International Journal, DOI:10.1080/08957959.2012.700308

To link to this article: <http://dx.doi.org/10.1080/08957959.2012.700308>



PLEASE SCROLL DOWN FOR ARTICLE

Full terms and conditions of use: <http://www.tandfonline.com/page/terms-and-conditions>

This article may be used for research, teaching, and private study purposes. Any substantial or systematic reproduction, redistribution, reselling, loan, sub-licensing, systematic supply, or distribution in any form to anyone is expressly forbidden.

The publisher does not give any warranty express or implied or make any representation that the contents will be complete or accurate or up to date. The accuracy of any instructions, formulae, and drug doses should be independently verified with primary sources. The publisher shall not be liable for any loss, actions, claims, proceedings, demand, or costs or damages whatsoever or howsoever caused arising directly or indirectly in connection with or arising out of the use of this material.

## The structural and optical properties of ZnO bulk and nanocrystals under high pressure

A. Duzynska<sup>a</sup>, R. Hrubciak<sup>b</sup>, V. Drozd<sup>b</sup>, H. Teisseyre<sup>a,c,\*</sup>, W. Paszkowicz<sup>a</sup>, A. Reszka<sup>a</sup>,  
A. Kaminska<sup>a</sup>, S. Saxena<sup>b</sup>, J.D. Fidelus<sup>a,c</sup>, J. Grabis<sup>d</sup>, C.J. Monty<sup>e</sup>, A. Suchocki<sup>a,f</sup>

<sup>a</sup>Institute of Physics, Polish Academy of Sciences, Lotników 32/46, 02-668 Warsaw, Poland; <sup>b</sup>CeSMEC, Florida International University, University Park, Miami, FL 33199, USA; <sup>c</sup>Institute of High Pressure Physics, Polish Academy of Science, Sokolowska 29/37, 01-142 Warsaw, Poland; <sup>d</sup>Institute of Inorganic Chemistry, Riga Technical University, 34 Miera, LV-2169 Salaspils, Latvia; <sup>e</sup>CNRS Laboratoire Procedes, Matériaux et Energie Solaire (PROMES), Odeillo, 66120 Font-Romeu, France; <sup>f</sup>Institute of Physics, Kazimierz Wielki University, Plac Weyssenhoffa 11, 85-072 Bydgoszcz, Poland

(Received 5 April 2012; final version received 1 June 2012)

The elastic properties of high-quality ZnO crystals and nanopowder of grain size of about 65 nm are studied for both wurtzite (low pressure) and rock-salt high pressure phases. The measured values of bulk moduli for wurtzite and rock-salt phases of bulk ZnO crystals are equal to  $156 \pm 13$  and  $187 \pm 20$  GPa, respectively, and considerably larger for ZnO nanocrystals. The phase transition begins at a pressure of about 9 GPa and it is completed at a pressure of about 13.8 GPa for bulk crystals, whereas the values of pressure at which the phase transition occurs are lower for nanocrystals. A careful Rietveld analysis of the obtained data does not exhibit the presence of any intermediate phases between low pressure wurtzite and high pressure rock-salt phases of ZnO. The phase transition is accompanied by a strong decrease in the near-band-gap photoluminescence intensity. In addition, the pressure coefficient of the near-band-gap luminescence in ZnO nanocrystals exhibits strong deviation from the linearity observed in bulk crystals. An analysis of the results shows that defects present in the nanopowdered sample are responsible for the observed effects.

**Keywords:** zinc oxide; phase transition, diamond anvil cell, X-ray diffraction.

### Introduction

The zinc oxide, zinc magnesium oxide and zinc cadmium oxide compounds have gained substantial interest in recent years. Zinc oxide is a direct wide band-gap semiconductor material ( $E_g = 3.37$  eV) with a large exciton binding energy of 60 meV for the bulk crystal, which could be easily increased in a quantum wells system. ZnO is nearly lattice matched to GaN, which makes this material attractive for future developments of optoelectronic, spintronic, and sensor application. ZnO in the polycrystalline form is commonly used in industry for producing pigments in paints, rubber, sunscreens and sunblocks, varistors and medicines. However, it is not easy to grow large ZnO monocrystals of good quality due to many defects that occur in bulk crystals. Among the defects that are observed in this material, the oxygen vacancies are the most common [1,2].

\*Corresponding author. Email: teiss@ifpan.edu.pl

The structural properties of ZnO crystals under hydrostatic pressure have already been studied for many years [3–14]. It is known that at hydrostatic pressures of about 9–13 GPa the phase transition from wurtzite (B4) to rock-salt (B1) phase occurs. Interesting behavior of this phase transition was predicted by Saitta and Decremps [15] and by Boulefffel and Leoni [16]. Their theoretical calculation predicts that an intermediate tetragonal or a hexagonal intermediate phase should appear between the B4 and B1 phases. One of the major goals of this paper was to search for such intermediate phases in the single crystals of very high quality and in nanocrystals with lower structural perfection, characteristic for this type of material. Established values of bulk moduli for both phases are quite scattered and vary from about 135 GPa [3] to about 183 GPa [4] for the wurtzite phase and from 132 GPa [7] to about 228 GPa [4] for rock-salt phase (see also Table I in Ref. [3]). One of the possible reasons for such a large scattering of the values of bulk moduli could be associated with the quality of the sample material. Samples could contain a large number of intrinsic defects that are difficult to control. The phase transition pressure and the existence of the intermediate phase between the B4 and B1 phases can also be related to the sample quality and the existence of a uniaxial pressure components in the pressure-transmitting medium (PTM). In this paper we would like to compare the elastic properties under high hydrostatic pressure of very good quality bulk ZnO crystals with those of ZnO nanocrystals prepared by evaporation of coarse-grained commercially available oxide powder into a radio-frequency air plasma and nanostructured with solar physical vapor deposition (SPVD) process or by vaporization–condensation in the solar furnace [17]. The pressure-induced phase transitions strongly affect luminescence properties of ZnO crystals, effectively quenching bulk crystal luminescence and broadening luminescence emitted from nanocrystalline samples.

The small size nanocrystalline powders of various II–VI semiconductors have different elastic properties under pressure than bulk crystals. Nanocrystallization changes the pressure at which the phase transition occurs, which is an effect of surface tension and surface energy difference between the phases involved [18,19]. It also may affect the reversibility of the phase transition, for example, it has been found that the cubic phase in 12 nm nanocrystalline powders can be preserved even at ambient pressure after pressure release. However, the influence of nanocrystallization on the structural properties of the crystals can be observed only when the surface tension is strong enough to create relatively large pressure inside the crystal. This means that this effect can be important only for small nanoparticles, with size of the order of 10 nm.

## Samples and experiment

Bulk crystals of ZnO can be grown by different techniques such as vapor phase transport, hydrothermal and pressure melt method. The largest crystals have been obtained by a hydrothermal method. In this method, an aqueous solution together with a KOH and LiOH are used as a solvent for ZnO seeds. Unfortunately, the hydrothermal crystals incorporate alkali metals, mostly K and Li, and small amounts of metallic impurities from the autoclave. A common method to produce very high-quality ZnO crystals wafers is based on vapor transport; however, in this case dimensions of crystals which can be obtained are limited to a few centimeters.

Remarkably large ZnO crystals, up to 2 kg in weight, have been found during industrial production of zinc white in Olawa Foundry in Olawa, Poland. Properties of these crystals have been reported elsewhere only once and have been looked at as rather a mineralogical curiosity [20]. Industrial production of zinc white in Olawa Foundry is performed by a method known as the French process. The system consists of two chambers, the upper part being the combustion chamber where natural gas is burned to produce heat. The chambers are separated by a ceramic diaphragm. In the upper chamber, the temperature rises to about 1500°C. Metallic zinc is melted

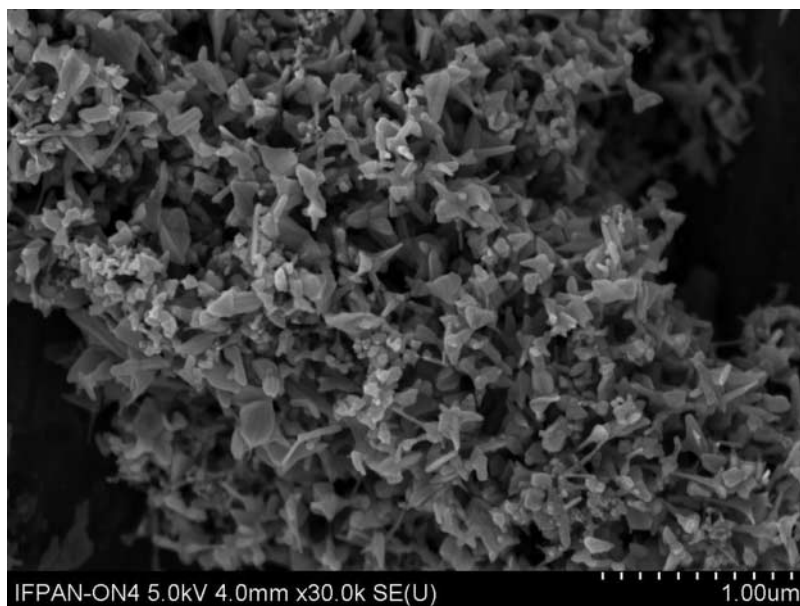


Figure 1. Photograph taken by scanning electron microscope (SEM) of nano-crystalline ZnO after the SPVD process in the solar reactor.

and vaporized in a bottom chamber at a temperature above  $907^{\circ}\text{C}$ . Zinc vapor is overheated to  $950^{\circ}\text{C}$  and leaves the chamber into the oxidation chamber where it instantaneously reacts with the oxygen in the air to give ZnO particles with an average size of a few micrometers. A periodic shutdown of the facility for physical inventory verification reveals that the diaphragm and vaporization chamber are covered by remarkably large ZnO crystals. Due to fact that these large ZnO crystals have excellent optical properties, described in the next part of this paper, samples of this material were used in our high pressure experiments.

The nanocrystalline ZnO samples were prepared by evaporation of mixtures of coarse-grained oxides in an inductively coupled plasma. The obtained ZnO powder with a grain size of about  $1\ \mu\text{m}$  was subsequently nanostructured by SPVD with the use of a Heliotron sun reactor in the High Flux Solar Facilities at the CNRS Laboratoire Procédés, Matériaux et Énergie Solaire (PROMES), Odeillo/Font Romeu (France). The  $1\ \mu\text{m}$  grained ZnO powder was pressed into small pellets and placed in the sun reactor in a vacuum glass chamber. The sample was illuminated by the focused sunlight with a power density of about  $730 \pm 100\ \text{W}/\text{cm}^2$ . The sample undergoes sunlight ablation and is deposited by condensation on a water-cooled copper tube ('cold finger') located a few centimeters above the target and on a ceramic filter. The product is finally scratched from the filter. Photograph taken by scanning electron microscope (SEM) of the powder is shown in Figure 1. The details of the process are described in References [21,22].

The photoluminescence (PL) spectra of ZnO samples were obtained using a 325-nm (3.81 eV) line of a He–Cd 15 mW laser as the excitation source. The spectra were measured with the use of a Horiba Jobin-Yvon FHR 1000 monochromator with a charge-coupled device detector. The spectra were corrected for the quantum efficiency of the detector. The high pressure measurements were performed with use of a low-temperature diamond anvil cell (DAC) (Diacell Products MCDAC-2) loaded with argon as a PTM. The DAC was mounted into an Oxford Optistat CF cryostat and measurements were performed at 11 K. The *R1* ruby luminescence line was used for pressure measurements. Polished samples of bulk ZnO crystals of thickness about  $30\ \mu\text{m}$  or ZnO

nanopowder were loaded into the cell along with a small piece of ruby. The changes of pressure were performed at room temperature in order to minimize non-hydrostatic effects.

X-ray diffraction (XRD) measurements of bulk crystalline ZnO were conducted on the beamline IDB-16 ( $\lambda = 0.3981 \text{ \AA}$ ) of the Advanced Photon Source (APS) at Argonne National Laboratory. Diffracted X-rays were collected at Bragg angles of up to  $2\Theta = 25^\circ$  using a MAR3450 imaging detector. One series of measurements for bulk ZnO crystal was performed in neon gas as a PTM in order to check the effects of possible non-hydrostaticity. The results obtained in neon and in poly(dimethylsiloxane) (silicone oil, viscosity 5cSt) are consistent with each other, which means that the effects of non-hydrostaticity are rather weak and similar for both used PTM. Symmetrical-type DAC with 300  $\mu\text{m}$  culet diameter diamonds was used for measurements with neon and a Mao-Bell-type DAC with 400  $\mu\text{m}$  culet diameter diamonds was used for measurements with silicone oil.

XRD measurements of ZnO nanopowder under pressures of up to 15 GPa were conducted using an MAR3450 imaging detector on B2 beamline ( $\lambda = 0.48595 \text{ \AA}$ ) at Cornell High Energy Synchrotron Source (CHESS). Measurements at high pressure were carried out using the DAC of Mao-Bell [23] type with 400  $\mu\text{m}$  culet diameter diamonds. Typical exposure times for XRD collection were in the range between 450 and 600 s. Silicone oil was used as a hydrostatic PTM.

Sample to detector distance and other diffraction geometry parameters were calibrated using a  $\text{CeO}_2$  standard. 2D angle-dispersive diffraction images were processed using the software FIT2D [24] to generate the intensity *vs.* two-theta diffraction patterns. Each diffraction peak was fitted with a pseudo-Voigt function using FITYK software [25] to obtain its  $2\Theta$  angle. To determine the *a* and *c* lattice parameters of the *wurtzite* phase of ZnO, *d*-spacings of diffraction peaks (100), (002), (101), (102), (110) and (103) were fitted using least squares to a hexagonal lattice. Lattice parameter of the cubic *NaCl*-phase ZnO was determined using an arithmetic average of *d*-spacings of diffraction peaks (111), (200), (220), (311) and (222). Platinum was used as an *in situ* pressure marker. Similarly, the lattice parameter of the platinum pressure marker was calculated using four non-overlapping diffraction peaks – (111), (200), (220) and (311). The pressure was calculated using an equation of state of platinum proposed by Fei et al. [26]

## Results and discussion

Figure 2 illustrates the emission spectra of the bulk crystals of ZnO at a temperature of 14 K and ambient pressure in comparison with the nanocrystalline sample. In the case of bulk crystals at low temperatures, the PL spectra are dominated by sharp lines that can be attributed to excitons bound on unidentified neutral donors. The low value of full-width at half-maximum (of 0.5 meV) reveals the high crystalline quality of this crystal. At higher energy, observed peaks were probably due to the excited state transition of exciton A (3.3776 eV), excitons bound on unidentified neutral donors related to exciton B (3.3731 eV) and rotator states (3.3659 and 3.3664 eV). The identification of an excitonic lines follows the results from fundamental excitonic region, published by Teke et al. [27].

The near-band-gap low-temperature emission of nanocrystalline ZnO forms a broad band with a maximum at about 3.3 eV, showing some unresolved bands, most probably associated with bound excitons luminescence and some phonon replicas of the exciton lines. In addition to that a weaker broad-band defect ZnO luminescence is visible in these samples with two maxima at 2.39 and 3.08 eV. Only very weak defect luminescence at about 2.4 eV is observed in our bulk crystals. Apparently, nanocrystalline samples do not exhibit the same excellent optical properties as bulk ZnO crystals. Some stress and defects existing in small nanocrystals may contribute to the broadening of the luminescence of nanocrystalline sample as compared with the bulk material [18,19,28].

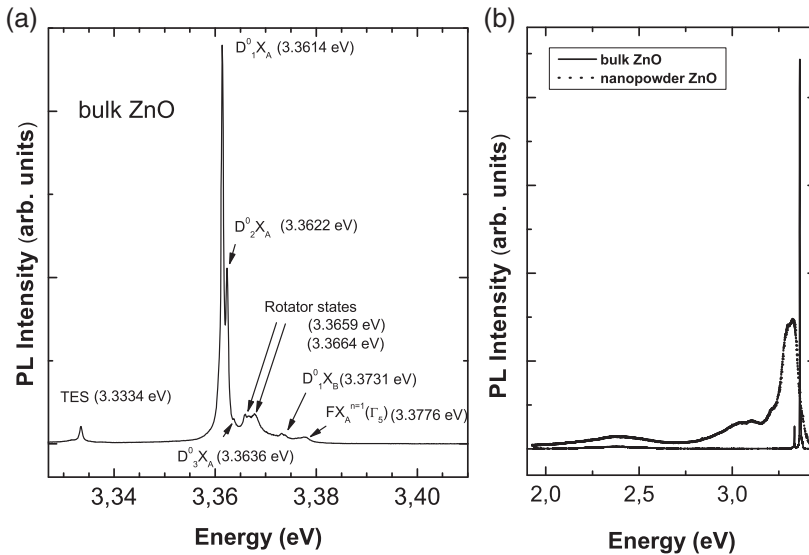


Figure 2. Ambient-pressure luminescence spectra of bulk and nano-crystalline ZnO samples at  $T = 14$  K. (a) high-resolution luminescence spectrum of bulk ZnO sample at region of exciton emission (TES – two electron satellite) and (b) a comparison of luminescence of bulk and nano-crystalline samples.

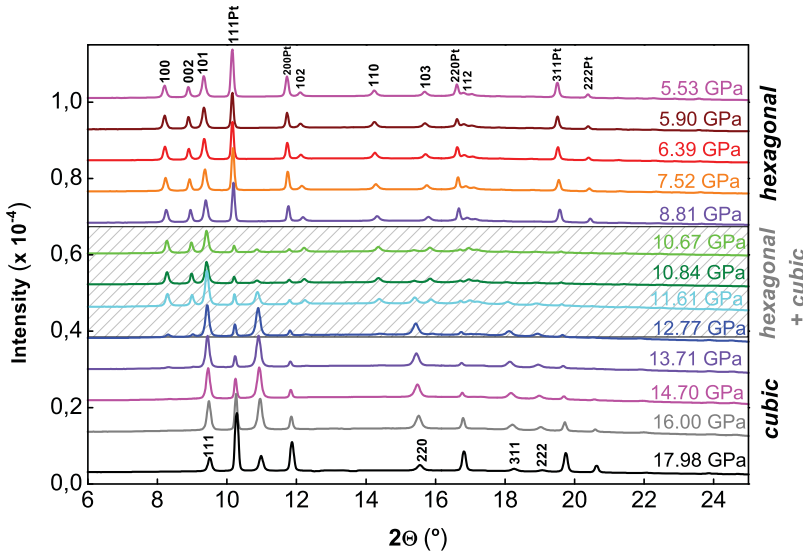


Figure 3. XRD spectra for ZnO bulk crystal as a function of pressure at room temperature with neon as PTM. The shaded area shows coexistence of wurtzite (hexagonal) and rock-salt (cubic) phases.

The results of XRD measurements of bulk ZnO sample in neon as a PTM for pressures between 5.53 and 17.98 GPa are presented in Figure 3. The data show that the crystal undergoes a pressure-induced phase transition at a pressure of about 9 GPa from the B4 wurtzite phase to the B1 rock-salt phase. The pure rock-salt phase is observed above pressures of 13.8 GPa. Between 9 and 13.8 GPa both phases co-exist. At the phase transition, the volume per formula unit (p.f.u.) undergoes a large collapse, from around 22.4 down to 18.6 Å<sup>3</sup>. The dependence of the volume p.f.u. as a function of pressure is shown in Figure 4 for bulk ZnO and ZnO nanocrystals. Two series of measurements were conducted for bulk ZnO crystals with neon and silicon oil as PTM.

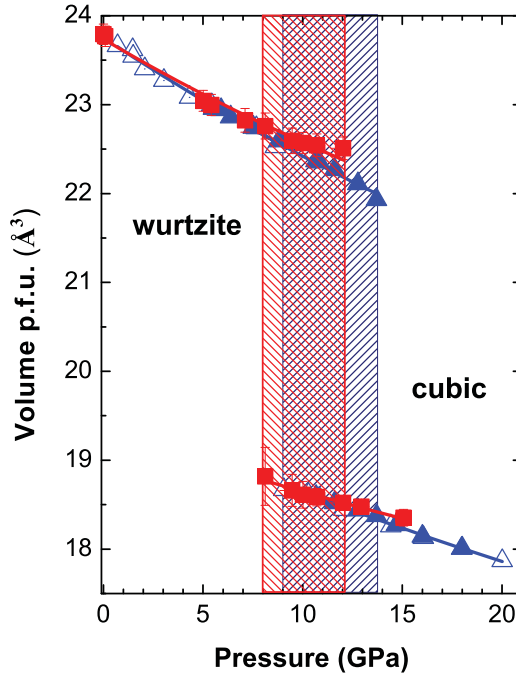


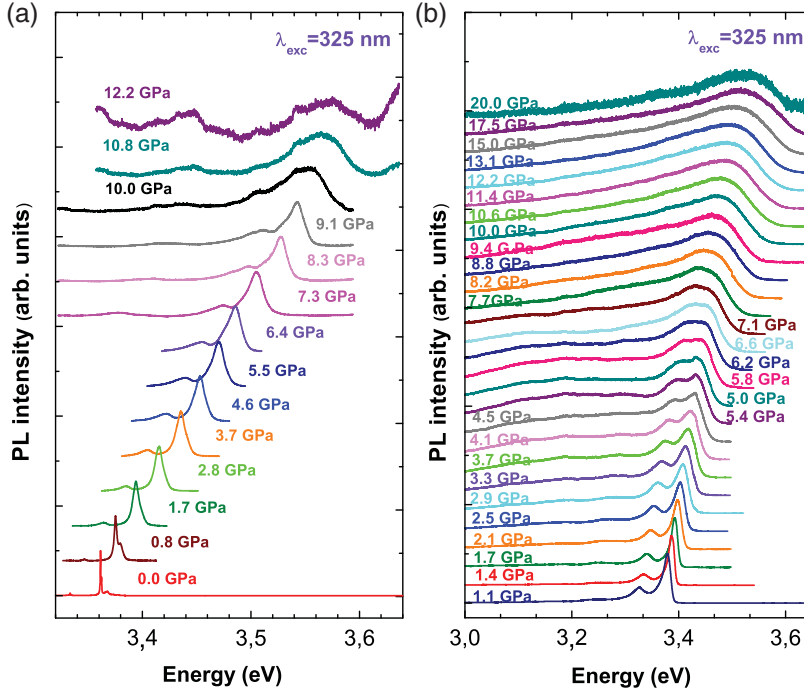
Figure 4. The pressure dependence of the volume p.f.u. for bulk and nano-crystalline ZnO. Triangles (blue on line) – bulk ZnO sample. Open symbols: data taken with silicon oil as a PTM, solid symbols: with neon as a PTM. Squares (red on line) – ZnO nanopowder. The shaded areas are the pressure ranges for which both phases coexist. These ranges are different for bulk and nano-crystalline samples, for nano-crystalline ZnO this range is shifted to lower pressures. Lines: fits of Murnaghan equation of state.

Both series of measurements yielded very similar results and they are treated together in further analysis. The solid lines in Figure 4 are the fits of Murnaghan [29] equation of state to the data for both wurtzite and cubic phases. The fits yield values of bulk moduli and their pressure derivatives, listed in Table 1. Obtained values of bulk moduli for low and high pressure phases of ZnO *bulk samples* are in the middle of results reported up to now (between 135 and 183 GPa, according to References [3,4], for the B4 phase, and between 132 GPa [7] and 228 GPa [4] for the B1 phase). Taking into account very good quality of our bulk ZnO crystal, we consider that the obtained results are the most reliable. The defects in crystals (both intrinsic and extrinsic) may change the structural stability of the crystals, changing the pressure range at which the phase transition occurs, as it was observed in the case of LiNbO<sub>3</sub> crystals with different stoichiometries [30]. Obtained values of bulk modulus of the wurtzite phase of bulk crystals are in very good agreement with theoretical calculations, presented in Reference [12]. The measured bulk modulus for rock-salt phase agrees very well with theoretical estimations of Liu et al. [3]; however, relatively large error bars resulting from the small number of experimental points encompass several other theoretical estimations [3–13].

Different results are obtained for nanopowdered ZnO samples. They appear to be considerably less compressible than bulk crystals for both low and high pressure phases, as it can be seen from Table 1. Other types of ZnO nanoparticles such as nanowires and nanobelts exhibit a similar behavior. Also the phase transition region is different for the nanocrystals and extends from 8 to 12 GPa. For small nanocrystals, such a result could be associated with surface effects, *i.e.* the influence of surface tension of the nanopowdered samples [18]. Surface tension decreases the pressure at which phase transition occurs, and also increases bulk moduli of both phases. However, the average size of nanocrystals in our sample (65 nm) cannot explain such a behavior

Table 1. Bulk moduli, their pressure derivatives and volumes p.f.u. for bulk and nanopowder ZnO at room temperature.

	Wurtzite phase		Rocksalt phase	
	ZnO crystal	ZnO nanopowder	ZnO crystal	ZnO nanopowder
Bulk modulus $B_0$ (GPa)	$156 \pm 13$	$184 \pm 22$	$187 \pm 20$	$260 \pm 30$
Pressure derivative of bulk modulus $B_0$	$3.3 \pm 1$	$4.0 \pm 1$	$3.4 \pm 1.5$	$3.5 \pm 2$
Volume per formula unit ( $\text{\AA}^3$ )	$23.78 \pm 0.03$	$23.72 \pm 0.05$	$19.57 \pm 0.04$	$19.33 \pm 0.08$

Figure 5. Normalized PL spectra as a function of pressure at  $T = 11$  K of (a) bulk ZnO crystal and (b) ZnO nano-crystalline sample.

unless the actual size of the nanoparticles is much smaller than that observed by SEM, *i.e.* large complexes of much smaller nanocrystals are observed in SEM [31]. Relatively large amount of defects present in our nanocrystalline samples may be another source of this effect.

Special attention has been paid to the analysis of the phase transition region in order to search for the postulated intermediate phase. However, a careful Rietveld analysis of that pressure region did not reveal any signature of any additional phases in both types of ZnO samples studied. Neither good quality of the bulk sample and small non-hydrostaticity nor the increased number of defects in the nanocrystalline sample does not contribute to the formation of such additional phases in the studied ZnO samples.

The phase transitions profoundly modify PL properties of ZnO samples. Figure 5 presents results of high pressure PL measurements of both types of the samples at  $T = 11$  K. For the bulk sample (Figure 5(a)), a relatively sharp luminescence in the region of band-gap energies is observed up to about 9 GPa. Above that pressure, the luminescence became very broad, and finally completely disappears for pressure above 12 GPa. This very well agrees with the XRD results, apparently above 12 GPa, the amount of the wurtzite phase is very small and it is not detected in the luminescence.

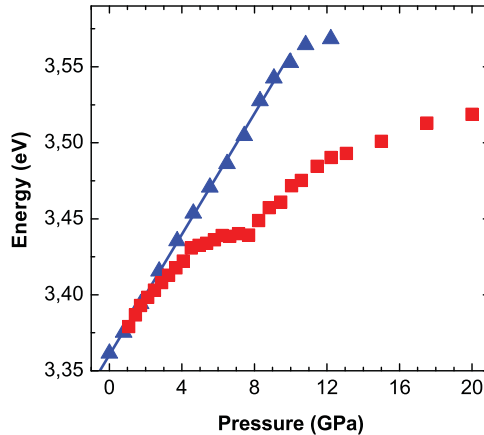


Figure 6. Pressure dependencies of the position of the maxima of PL for bulk (triangles) and nano-crystalline (squares) ZnO samples at  $T = 11$  K.

A different behavior is observed for the nanocrystalline sample, presented in Figure 5(b). A relatively sharp luminescence is observed only up to pressure of about 6 GPa. For higher pressures, the sharp luminescence structure becomes gradually much broader. Also two component peaks of different luminescence intensities can be observed in the spectra: one with lower energy and intensity at low pressures (at an energy of about 3.26 eV at a pressure of 1.1 GPa), and the second one with higher energy and higher intensity at low pressure (at an energy of about 3.29 eV at a pressure of 1.1 GPa). Above pressures of 8 GPa, the sharp structure is replaced by a broad band in the region of the band-gap. This change is also accompanied by a strong decrease in the luminescence efficiency under 325 nm excitation.

The positions of the maxima of the luminescence as a function of pressure for both samples are shown in Figure 6. The bulk sample luminescence maximum shifts with pressure linearly with pressure coefficient equal to about 19.9 meV/GPa. The nanocrystalline sample exhibits a different behavior: at low pressures up to about 3 GPa luminescence peak shifts linearly with a pressure coefficient being the same as for the bulk sample. At higher pressures, the luminescence peak increases its energy non-linearly and with a much slower rate than in the bulk sample. There is also an apparent kink in this dependence, at a pressure of 8 GPa, at which XRD data show appearance of rock-salt phase for this sample. Possibly, this is an effect of the relative changes of the luminescence intensity in two major peaks observed in the nanocrystalline sample. With increase in pressure, the lower energy peak becomes dominating over the higher energy luminescence peak, having higher intensity at low pressures.

It remains unclear why it is possible to observe luminescence above the phase transition pressure in the nanocrystalline sample. The high pressure B1 phase of ZnO is supposed to have indirect band-gap. Therefore, the luminescence should be quenched, as it is observed in the bulk sample. Contrary to what is observed in the nanocrystalline sample, up to about at least 20 GPa. A similar result was observed earlier in ZnO nanosheets [32].

## Summary and conclusions

The lack of reliable values of bulk modulus of ZnO was the motivation for measurements of the elastic properties of this compound using very good-quality ZnO crystals. A subsequent goal of this paper was to compare the compressibility of very good-quality bulk ZnO with the compressibility of ZnO nanocrystals. The values of bulk moduli for wurtzite (hexagonal) and rock-salt (cubic)

phases, established in this work, are equal to  $156 \pm 13$  and  $187 \pm 20$  GPa, respectively. These values are considerably larger for ZnO nanocrystals. These results show the influence of grain size and crystal quality of the nanocrystalline samples of ZnO on their elastic properties [33]. The phase transition from wurtzite to cubic phase is observed in the pressure region between 9.5 and 13.8 GPa for bulk crystals and at slightly lower pressures for nanocrystalline ZnO. Contrary to theoretical expectations [15], no additional intermediate phase of ZnO was detected, neither for bulk nor for nanocrystalline samples.

The phase transition quenches the near-band-gap luminescence of ZnO in bulk crystals. In ZnO nanocrystals, occurrence of the phase transition strongly broadens the near-band-gap luminescence and decreases its efficiency. In addition, the pressure coefficient of the luminescence maximum in nanocrystalline ZnO considerably deviates from the linear dependence observed for bulk ZnO.

## Acknowledgements

This work was partially supported by the European Union within the European Regional Development Fund through the Innovative Economy grant MIME (POIG.01.01.02-00-108/09) and by the project "Nanomaterials for renewable energy applications" (RENANOS, 2010) within the framework of the EU-DG RTD's "Solar Facilities for the European Research Area (SFERA)". This work was supported in part by the DOE/NNSA through the Carnegie/DOE Alliance Center (cooperative agreement DE-FC52-08NA28554).

Portions of this work were performed at HPCAT (Sector 16), APS, Argonne National Laboratory. HPCAT is supported by CIW, CDAC, UNLV, and LLNL through funding from DOE-NNSA, DOE-BES, and NSF. Compressed neon gas loading was performed at GeoSoilEnviroCARS (Sector 13), APS, Argonne National Laboratory. GeoSoilEnviroCARS is supported by the National Science Foundation – Earth Sciences (EAR-0622171) and Department of Energy – Geosciences (DE-FG02-94ER14466). APS is supported by DOE-BES, under Contract No. DE-AC02-06CH11357. In the USA this work was supported in part by the DOE/NNSA through the Carnegie/DOE Alliance Center (cooperative agreement DE-FC52-08NA28554).

Portions of this work are based upon research conducted at the CHESS which is supported by the National Science Foundation and the National Institutes of Health/National Institute of General Medical Sciences under NSF award DMR-0936384.

## References

- [1] C. Klingshirn, J. Fallert, H. Zhou, J. Sartor, C. Thiele, F. Maier-Flaig, D. Schneider, and H. Kalt, *Phys. Status Solidi B* 247 (2010), pp. 1324–1447.
- [2] M.D. McCluskey and S.J. Jokela, *J. Appl. Phys.* 106 (2009), 071101.
- [3] H. Liu, Y. Ding, M. Somayazulu, J. Qian, J. Shu, D. Hausermann, and H.K. Mao, *Phys. Rev. B* 71 (2005), pp. 212103-1–4 and references therein.
- [4] H. Karzel, W. Potzel, M. Kofferlein, W. Schiessl, M. Steiner, U. Hiller, G.M. Kalvius, D.W. Mitchell, T.P. Das, P. Blaha, K. Schwarz, and M.P. Pasternak, *Phys. Rev. B* 53 (1996), pp. 11425–11438.
- [5] L. Gerward and J.S. Olsen, *J. Synchrotron Radiat.* 2 (1995), pp. 233–235.
- [6] S. Desgreniers, *Phys. Rev. B* 58 (1998), pp. 14102–14105.
- [7] J.M. Recio, M.A. Blanco, V. Luana, R. Pandey, L. Gerward, and J.S. Olsen, *Phys. Rev. B* 58 (1998), pp. 8949–8954.
- [8] F. Decremps, J. Zhang, and R. Lieberman, *Europhys. Lett.* 51 (2000), pp. 268–274.
- [9] F. Decremps, F. Datchi, A.M. Saita, A. Polian, S. Pascarelli, A. Di Cicco, J.P. Itie, and F. Baudelet, *Phys. Rev. B* 68 (2003), pp. 104101-1-10.
- [10] Y. Mori, N. Niiya, K. Ukegawa, T. Mizuno, K. Takarabe, and A. Ruoff, *Phys. Stat. Sol. B* 241 (2004), pp. 3198–3202.
- [11] R. Ahuja, L. Fast, O. Eriksson, J.M. Wills, and B. Johansson, *J. Appl. Phys.* 83 (1998), pp. 8065–8067.
- [12] J.E. Jaffe and A.C. Hess, *Phys. Rev. B* 48 (1993), pp. 7903–7909.
- [13] J.E. Jaffe, J.A. Snyder, Z. Lin, and A.C. Hess, *Phys. Rev. B* 62 (2000), pp. 1660–1665.
- [14] A. Segura, J.A. Sans, D. Erandonea, D. Martinez-Garcia, and F. Fages, *Appl. Phys. Lett.* 88 (2006), pp. 011910-1-3.
- [15] A. Marco Saitta and F. Decremps, *Phys. Rev. B* 70 (2004), pp. 035214-1-5.
- [16] S.E. Boulfelfel and S. Leoni, *Phys. Rev. B* 78 (2008), pp. 125204-1-7.
- [17] A. Ahecene, C. Monty, J. Kouam, A. Thorel, G. Petot-Ervias, and A. Djemel, *J. Eur. Ceram. Soc.* 27 (2007), pp. 3413–3424.
- [18] S.H. Tolbert and A.P. Alivisatos, *Z. Phys. D* 26 (1993), pp. 56–58.
- [19] J.Z. Jiang, J.S. Olsen, L. Gerward, D. Frost, D. Rubie, and J. Peyronneau, *Europhys. Lett.* 50 (2000), pp. 48–53.
- [20] J.W. Nowak, R.S.W. Braithwaite, J. Nowak, K. Ostojski, M. Krystek, W. Buchowiecki, *J. Gemmol.* 30 (2007), pp. 257–267.

- [21] A. Kalinko, J.D. Fidelus, L. Grigorjeva, D. Millers, C.J. Monty, A. Presz, and K. Smits, *J. Phys.: Conf. Ser.* 93 (2007), pp. 012044-1-6.
- [22] L. Grigorjeva, D. Millers, V. Pankratov, A. Kalinko, J. Grabis, C. Monty, *J. Phys.: Conf. Ser.* 93 (2007), pp. 012036-1-8.
- [23] A. Jayaraman, *Rev. Sci. Instrum.* 57 (1986), pp. 1013–1031.
- [24] A. Hammersley, Available at <http://www.esrf.eu/computing/scientific/FIT2D/> (2009).
- [25] M. Wojdyr, *J. Appl. Crystallogr.* 43 (2010), pp. 1126–1128.
- [26] Y. Fei, A. Ricolleau, M. Frank, K. Mibe, G. Shen, and V. Prakapenka, *Proc. Natl. Acad. Sci. U.S.A.* 104 (2007), pp. 9182–9186.
- [27] A. Teke, Ü. Özgür, S. Doğan, X. Gu, H. Morkoç, B. Nemeth, J. Nause, and H.O. Everitt, *Phys. Rev. B* 70 (2004), pp. 195207-1-10.
- [28] J.D. Fidelus, A. Karbowski, J. Grabis, A. Jusza, R. Piramidowicz, R.S. Brusa, and G.P. Karwasz, *Acta Phys. Pol. A* 120 (2011), A-66–68.
- [29] F.D. Murnaghan, *Proc. Natl. Acad. Sci. U.S.A.* 30 (1944), pp. 244–247.
- [30] A. Suchocki, W. Paszkowicz, A. Kamińska, A. Durygin, S.K. Saxena, L. Arizmendi, and V. Bermudez, *Appl. Phys. Lett.* 89 (2006), pp. 261908-1-3.
- [31] M. Baran, Ya. Zhydachevskii, A. Suchocki, A. Reszka, S. Warchol, R. Diduszko, and A. Pajaczkowska, *Opt. Mater.* 34 (2012), pp. 604–608.
- [32] S.J. Chen, Y.C. Liu, C.L. Shao, C.S. Xu, Y.X. Liu, L. Wang, B.B. Liu, and G.T. Zou, *J. Appl. Phys.* 98 (2005), pp. 106106-1-3.
- [33] F. Decremps, J. Pellicer-Porres, F. Datchi, J.P. Itie, A. Polian, and F. Baudalet, *Appl. Phys. Lett.* 81 (2002), pp. 4820-1-3.